

# **GMPR: A robust normalization method for zero-inflated count data with application to microbiome sequencing data**

**Li Chen**<sup>1</sup>, **James Reeve**<sup>2</sup>, **Lujun Zhang**<sup>3</sup>, **Shengbing Huang**<sup>2</sup>, **Xuefeng Wang**<sup>4</sup>, **Jun Chen**<sup>Corresp. 2, 5</sup>

<sup>1</sup> Department of Health Outcomes Research and Policy, Harrison School of Pharmacy, Auburn University, Auburn, Alabama, United States

<sup>2</sup> Bioinformatics and Computational Biology Program, University of Minnesota - Rochester, Rochester, Minnesota, United States

<sup>3</sup> College of Environmental and Resource Sciences, Zhejiang University, Hangzhou, Zhejiang, China

<sup>4</sup> Department of Biostatistics and Bioinformatics, Moffitt Cancer Center, Tampa, Florida, United States

<sup>5</sup> Division of Biomedical Statistics and Informatics and Center for Individualized Medicine, Mayo Clinic, Rochester, Minnesota, United States

Corresponding Author: Jun Chen

Email address: chen.jun2@gmail.com

Normalization is the first critical step in microbiome sequencing data analysis used to account for variable library sizes. Current RNA-Seq based normalization methods that have been adapted for microbiome data fail to consider the unique characteristics of microbiome data, which contain a vast number of zeros due to the physical absence or under-sampling of the microbes. Normalization methods that specifically address the zero inflation remain largely undeveloped. Here we propose GMPR - a simple but effective normalization method - for zero-inflated sequencing data such as microbiome data. Simulation studies and real datasets analyses demonstrate that the proposed method is more robust than competing methods, leading to more powerful detection of differentially abundant taxa and higher reproducibility of the relative abundances of taxa.

# 1 **GMPR: A robust normalization method for** 2 **zero-inflated count data with application to** 3 **microbiome sequencing data**

4 **Li Chen<sup>1</sup>, James Reeve<sup>2</sup>, Lujun Zhang<sup>3</sup>, Shengbing Huang<sup>2</sup>, Xuefeng**  
5 **Wang<sup>4</sup>, and Jun Chen<sup>2, 5</sup>\***

6 <sup>1</sup>**Department of Health Outcomes Research and Policy, Harrison School of Pharmacy,**  
7 **Auburn University, AL 36849, USA**

8 <sup>2</sup>**Bioinformatics and Computational Biology Program, University of Minnesota,**  
9 **Rochester, MN 55905, USA**

10 <sup>3</sup>**College of Environmental and Resource Sciences, Zhejiang University, Zhejiang,**  
11 **310058, China**

12 <sup>4</sup>**Department of Biostatistics and Bioinformatics, Moffitt Cancer Center, Tampa, FL**  
13 **33612, USA**

14 <sup>5</sup>**Division of Biomedical Statistics and Informatics and Center for Individualized**  
15 **Medicine, Mayo Clinic, Rochester, MN 55905, USA**

16 **\*Corresponding addressed to: Chen.Jun2@mayo.edu**

## 17 **ABSTRACT**

18 Normalization is the first critical step in microbiome sequencing data analysis used to account for variable  
19 library sizes. Current RNA-Seq based normalization methods that have been adapted for microbiome  
20 data fail to consider the unique characteristics of microbiome data, which contain a vast number of  
21 zeros due to the physical absence or under-sampling of the microbes. Normalization methods that  
22 specifically address the zero-inflation remain largely undeveloped. Here we propose GMPR - a simple but  
23 effective normalization method - for zero-inflated sequencing data such as microbiome data. Simulation  
24 studies and real datasets analyses demonstrate that the proposed method is more robust than competing  
25 methods, leading to more powerful detection of differentially abundant taxa and higher reproducibility of  
26 the relative abundances of taxa.

## 27 **INTRODUCTION**

28 High-throughput sequencing experiments such as RNA-seq and microbiome sequencing are now routinely  
29 employed to interrogate the biological systems at the genome scale (Wang et al., 2009). After processing  
30 of the raw sequence reads, the sequencing data usually presents as a count table of detected features. The  
31 complex processes involved in the sequencing causes the sequencing depth (library size) to vary across  
32 samples, sometimes ranging several orders of magnitude. Normalization, which aims to correct or reduce  
33 the bias introduced by variable library sizes, is an essential preprocessing step before any downstream  
34 statistical analyses for high-throughput sequencing experiments (Dillies et al., 2013; Li et al., 2015).  
35 Normalization is especially critical when the library size is a confounding factor that correlates with the  
36 variable of interest. An inappropriate normalization method may either reduce statistical power with the  
37 introduction of unwanted variation, or more severely, result in falsely discovered features. One popular  
38 approach for normalizing the sequencing data involves calculating a size factor for each sample as an  
39 estimate of the library size. The size factors can be used to divide the read counts to produce normalized  
40 data (in the form of relative abundances), or to be included as offsets in count-based regression models  
41 such as DESeq2 (Love et al., 2014) and edgeR (Robinson et al., 2010) for differential feature analysis.  
42 One simple normalization method is TSS (Total Sum Scaling), which uses the total read count for each  
43 sample as the size factor. However, there are a couple undesirable properties for TSS. First, it is not robust  
44 to outliers, which are disproportionately large counts that do not reflect the underlying true abundance.  
45 Outliers have frequently been observed in sequencing samples due to technical artifacts such as preferential

46 amplification by PCR (Aird et al., 2011). Several outliers could lead to the overestimation of the library  
47 size if not properly addressed. Second, it creates compositional effects: non-differential features will  
48 appear to be differential due to the constant-sum constraint (Tsilimigras and Fodor, 2016; Mandal et al.,  
49 2015; Morton et al., 2017). Compositional effects are much stronger when the differential features are  
50 highly abundant or their effects are in the same direction (not balanced). An ideal normalization method  
51 should thus capture the invariant part of the count distribution and be robust to outliers and differential  
52 features.

53 Many normalization methods have been developed for sequencing data generally, and for RNA-Seq  
54 data in particular (Dillies et al., 2013; Li et al., 2015). These methods mostly rely on the assumption that  
55 the dataset to be normalized has a large invariant part and the majority of features do not change with  
56 respect to the condition under study. Robust statistics such as median and trimmed mean, which are not  
57 sensitive to a small set of differential features, are frequently used to estimate the library size. Two popular  
58 normalization methods for RNA-Seq data include TMM (Trimmed Mean of M values, implemented  
59 in edgeR) (Robinson and Oshlack, 2010) and the DESeq normalization (equivalent to Relative Log  
60 Expression normalization implemented in edgeR. For simplicity, we label it as “RLE”. ) (Anders and  
61 Huber, 2010). RLE method calculates the geometric means of all features as a “reference”, and all  
62 samples are compared to the “reference” to produce ratios (fold changes) for all features. The median  
63 ratio is then taken to be the RLE size factor. TMM method, on the other hand, selects a reference sample  
64 first, and all other samples are compared to the reference sample. The trimmed (weighted) mean of the  
65 log ratios is then calculated as the TMM size factor (log scale). Compared to RNA-Seq data, microbiome  
66 sequencing data are more over-dispersed and contain a vast number of zeros. Take the COMBO data  
67 for example (Wu et al., 2011), it contains 1,873 non-singleton OTUs (Operational Taxonomic Units, a  
68 proxy for bacterial species) from 99 samples and more than 80% of the OTU counts are zeros. Excessive  
69 zeros lead to a small number of “core” OTUs that are shared across samples. For the COMBO dataset,  
70 none of the OTUs are shared by all samples and only 5 OTUs are shared by more than 90% samples.  
71 For RLE, the geometric means of OTUs are not well defined for OTUs with 0s, and OTUs with 0s are  
72 typically excluded in size factor calculation. We are thus left with a very small number of common OTUs  
73 to calculate the size factor. As the OTU data become more sparse, RLE becomes less stable. For datasets  
74 like COMBO data, where there are no common OTUs, RLE fails. For TMM, a reference sample has  
75 to be selected before the size factor calculation. Reliance on a reference sample restricts the size factor  
76 calculation to a specific OTU set that the reference sample harbors (77 – 433 OTUs for COMBO data).  
77 Therefore, both RLE and TMM use only a small fraction of the data available in the OTU data and are not  
78 optimal from an information perspective.

79 One popular strategy to circumvent the zero-inflation problem is to add a pseudo-count (Mandal et al.,  
80 2015). This practice has a Bayesian explanation and implicitly assumes that all the zeros are due to  
81 under-sampling (McMurdie and Holmes, 2014). However, this assumption may not be appropriate due to  
82 the large extent of structural zeros due to physical absence. Moreover, the choice of the pseudo-count is  
83 very arbitrary and it has been shown that the clustering results can be highly dependent upon the choice  
84 (Costea et al., 2014). Recently, a new normalization method CSS (Cumulative Sum Scaling) has been  
85 developed for microbiome sequencing data (Paulson et al., 2013). In CSS, raw counts are divided by the  
86 cumulative sum of counts, up to a percentile determined using a data-driven approach. The percentile  
87 is aimed to capture the relatively invariant count distribution for a dataset. However, the determination  
88 of the percentiles could fail for microbiome datasets that have high count variability. Therefore, a more  
89 robust method to address the zero-inflated sequencing data is still needed.

90 Here we propose a novel inter-sample normalization method GMPR (Geometric Mean of Pairwise  
91 Ratios), developed specifically for zero-inflated sequencing data such as microbiome sequencing data. By  
92 comprehensive tests on simulated and real datasets, we show that GMPR outperforms the other competing  
93 methods for zero-inflated count data.

## 94 METHODS

### 95 GMPR normalization details

96 Our method extends the idea of RLE normalization for RNA-seq data and relies on the same assumption  
97 that there is a large invariant part in the count data. Assume we have a count table of OTUs from 16S  
98 rDNA targeted microbiome sequencing. Denote the  $c_{ki}$  as the count of the  $k$ th OTU ( $k = 1, \dots, q$ ) in the

99  $i$ th ( $i = 1, \dots, n$ ) sample. The RLE method calculates the size factor  $s_i$ , which estimates the (relative)  
100 library size of a given sample, based on

- Step 1: Calculate the geometric means for all OTUs

$$\mu_k^{GM} = (c_{k1}c_{k2} \cdots c_{kn})^{1/n}, k = 1, \dots, q$$

- Step 2: For a given sample,

$$s_i = \text{median}_k \{c_{ki}/\mu_k^{GM}\}, i = 1, \dots, n$$

Since geometric mean is not well defined for features with 0s, features with 0s are usually excluded in size calculation. However, for zero-inflated data such as microbiome sequencing data, as the sample size increases, the probability of existence of features without any 0s becomes smaller. It is not uncommon that a large dataset does not share any common taxa. In such cases, RLE fails. As an alternative, a pseudo-count such as 1 or 0.5 has been suggested to add to the original counts to eliminate 0s (Mandal et al., 2015). Since the majority of the counts may be 0s for microbiome data, adding even a small pseudo-count could have a dramatic effect on the geometric means of most OTUs. To circumvent the problem, GMPR reverses the order of the two steps of RLE. The first step is to calculate  $r_{ij}$ , which is the median count ratio of nonzero counts between sample  $i$  and  $j$ ,

$$r_{ij} = \underset{k \in \{1, \dots, q\} | c_{ki} \cdot c_{kj} \neq 0}{\text{Median}} \left\{ \frac{c_{ki}}{c_{kj}} \right\},$$

The second step is to calculate the size factor  $s_i$  for a given sample  $i$  as

$$s_i = \left( \prod_{j=1}^n r_{ij} \right)^{1/n}, i = 1, \dots, n.$$

101 Figure 1 illustrates the procedure of GMPR. The basic strategy of GMPR is that we conduct the  
102 pairwise comparison first and then combine the pairwise results to obtain the final estimate. Although  
103 only a small number of OTUs (or none) are shared across all samples due to severe zero-inflation, for  
104 every pair of samples, they usually share many OTUs. For example, 83 OTUs are shared on average  
105 for COMBO sample pairs. Thus, for pairwise comparison, we focus on these common OTUs that are  
106 observed in both samples to have a reliable inference of the abundance ratio between samples. We then  
107 synthesize the pairwise abundance ratios using a geometric mean to obtain the size factor. Based on this  
108 pair analysis strategy, we utilize far more information than RLE and TMM, both of which are restricted to  
109 a small subset of OTUs. It should be noted that GMPR is a general method, which could be applied to  
110 any type of sequencing data in principle.

111 The R implementation of GMPR could be accessed by [https://github.com/jchen1981/](https://github.com/jchen1981/GMP)  
112 GMPR.

### 113 Simulation studies to evaluate the performance of GMPR normalization

114 We study the performance of GMPR using simulated OTU datasets. Specifically, we study the robustness  
115 of GMPR to differential and outlier OTUs, and the effect on the performance of differential abundance  
116 analysis of OTU data. We compare GMPR to competing normalization methods including CSS, RLE,  
117 RLE+ (RLE with pseudo-count 1), TMM, TMM+ (TMM with pseudo-count 1) and TSS. The details of  
118 calculating the size factors using each normalization method are described in Box 1. The size factors  
119 from different normalization methods are further divided by the median so that they are on the same scale.

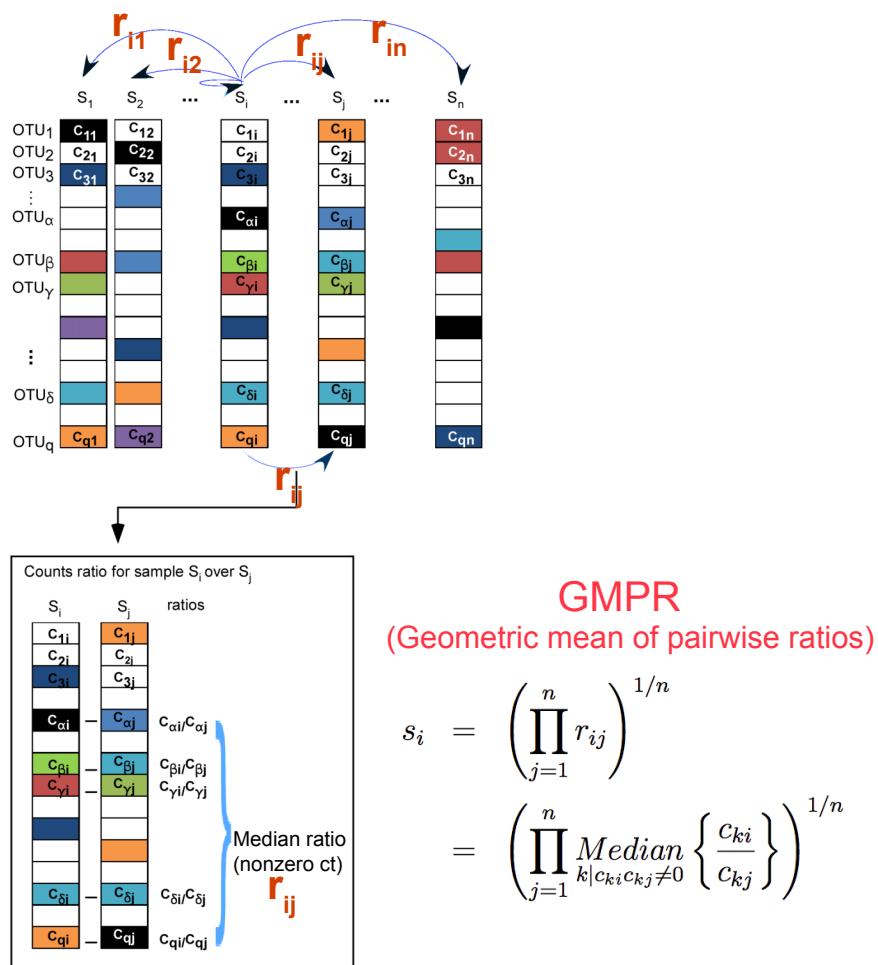


**Figure 1.** GMPR starts with pairwise comparisons (upper). Each pairwise comparison calculates the median abundance ratio of those common OTUs between the pair of samples (lower). The pairwise ratios are then synthesized into a final estimate.

**Box 1.** Calculation of size factors for normalization methods compared in the analysis.

- **GMPR (Geometric Mean of Pairwise Ratios):** The size factors for all samples are calculated by GMPR described in the Method section.
- **CSS (Cumulative Sum Scaling):** The size factors for all samples are calculated by applying `newMRExperiment`, `cumNorm` and `normFactors` in Bioconductor package `metagenome-Seq` (Paulson et al., 2013).
- **RLE (Relative Log Expression):** The size factors for all samples are calculated by the `calcNormFactors` with the parameter set as “RLE” in the edgeR Bioconductor package (Anders and Huber, 2010). The scaled size factors are obtained by multiplying the size factors with the total read count.
- **RLE+ (Relative Log Expression plus pseudo-counts):** The scaled size factors for all samples are calculated in the same way as RLE, except that each data entry is added with a pseudo-count 1.
- **TMM (Trimmed Mean of M values):** The size factors for all samples are calculated by the `calcNormFactors` function with the parameter set as “TMM” in the edgeR Bioconductor package (Robinson and Oshlack, 2010). The scaled size factors are obtained by multiplying the size factors with the total read count.
- **TMM+ (Trimmed Mean of M values plus pseudo-counts):** The scaled size factors for all sample are calculated in the same way as TMM, except that each data entry is added with a pseudo-count 1.
- **TSS (Total Sum Scaling):** The size factors are taken to be the total read counts.

120

#### 121 **Robustness to differential and outlier OTUs**

122 We first use a perturbation-based simulation approach to evaluate the performance of normalization  
 123 methods, focusing on their robustness to differentially abundant OTUs and sample-specific outlier OTUs.  
 124 The idea is that we first simulate the counts from a common probabilistic distribution so that the total  
 125 count is a proxy of the “true” library size. Next, we perturb the counts in different ways and apply  
 126 different normalization methods on the perturbed counts and evaluate the performance based on the  
 127 correlation between estimated size factor and “true” library size. Specifically, we generate zero-inflated  
 128 count data based on a Dirichlet-multinomial model with known library sizes (Chen and Li, 2013). The  
 129 mean and dispersion parameters of Dirichlet-multinomial distribution are estimated from the COMBO  
 130 dataset after filtering out rare OTUs with less than 10 reads and discarding samples with less than 1,000  
 131 reads ( $n=98, q=625$ ) (Wu et al., 2011). The library sizes are also drawn from those of the COMBO data.  
 132 To investigate the effect of sparsity (the number of zeros), OTU counts are simulated with different zero  
 133 percentages ( $\sim 60\%$ ,  $70\%$  and  $80\%$ ) by adjusting the dispersion parameter. A varying percentage of OTUs  
 134 ( $0\%$ ,  $1\%$ ,  $2\%$ ,  $4\%$ ,  $8\%$ ,  $16\%$ ,  $32\%$ ,  $64\%$ ) are perturbed in each set of simulation, with varying strength of  
 135 perturbation. The counts  $c_{ki}$  of perturbed OTUs are changed to  $\sqrt{c_{ki}}$  or  $c_{ki}^2$  for strong perturbation and  
 136  $0.25c_{ki}$  or  $4c_{ki}$  for moderate perturbation.

137 We employ two perturbation approaches where we decrease/increase the abundances of a “fixed” or  
 138 “random” set of OTUs. As shown in Figure 2, in the “fixed” perturbation approach, the same set of OTUs  
 139 are decreased/increased in the same direction for all samples, reflecting differentially abundant OTUs  
 140 under a certain condition such as disease state. In the “random” perturbation approach, each sample has a  
 141 random set of OTUs perturbed with a random direction, mimicking the sample-specific outliers.

142 Finally, size factors for all methods are estimated and the Pearson’s correlation between the estimated  
 143 and “true” library sizes is calculated. The simulation is repeated 25 times and the mean estimate and its  
 144 95% confidence intervals (CIs) are reported.

#### 145 **Effect on the performance of differential abundance analysis**

146 One use of the estimated size factor is for differential abundance analysis (DAA) of OTU data, where  
 147 the size factor (usually on a log scale) is included as an offset in a count-based parametric model to  
 148 address variable library sizes. Many count-based models have been proposed for differential abundance  
 149 analysis including DESeq2 and edgeR (McMurdie and Holmes, 2014). These methods usually come  
 150 with their native normalization schemes such as RLE for DESeq2 and TMM for edgeR. Therefore, it



**Figure 2.** Illustration of the simulation strategy. In the “fixed” perturbation approach, the abundances of the same set of OTUs are decreased/increased for all samples, reflecting differentially abundant OTUs under certain conditions such as disease state. In the “random” perturbation approach, each sample has a random set of OTUs perturbed with a random direction, reflecting the sample-specific outliers. The darkness of the color indicates the OTU abundance.

151 is interesting to see if the GMPR normalization could improve the performance of these methods. To  
 152 achieve this end, we use DESeq2 to perform DAA on the OTU table since DESeq2 has been shown to  
 153 be more robust than edgeR for zeroinflated dataset (Chen et al., 2018). We compare the performance of  
 154 DESeq2 using its native RLE normalization to that using GMPR or TSS normalization.

155 We use the same simulation strategy described in Chen et al. (2018). Specifically, Zero-inflated  
 156 Negative Binomial distribution (ZINB) is used to simulate the OTU count data. ZINB has the following  
 157 probability distribution function

$$f_{z\text{inb}}(c_{ki}|p_{ki}, \mu_{ki}, \phi_{ki}) = p_{ki} \cdot I_0(c_{ki}) + (1 - p_{ki}) \cdot f_{nb}(c_{ki}|\mu_{ki}, \phi_{ki}), \quad (1)$$

158 which is a mixture of a point mass at zero ( $I_0$ ) and a negative binomial ( $f_{nb}$ ) distribution of the form

$$f_{nb}(c_{ki}|\mu_{ki}, \phi_{ki}) = \frac{\Gamma(c_{ki} + \frac{1}{\phi_{ki}})}{\Gamma(c_{ki} + 1)\Gamma(\frac{1}{\phi_{ki}})} \cdot \left(\frac{\phi_{ki}\mu_{ki}}{1 + \phi_{ki}\mu_{ki}}\right)^{c_{ki}} \cdot \left(\frac{1}{1 + \phi_{ki}\mu_{ki}}\right)^{\frac{1}{\phi_{ki}}}. \quad (2)$$

The three parameters - prevalence( $p_{ki}$ ), abundance( $\mu_{ki}$ ) and dispersion( $\phi_{ki}$ ) - fully capture the zero-inflated and dispersed count data. We generate the simulated datasets (two sample groups of size 49 each) based on the parameter values estimated from the COMBO dataset. 5% of OTUs are randomly selected to have their counts in one group multiplied by a factor of 4. The groups in which this occurs are randomly selected and thus the abundance change is relatively “balanced”. To further study the performance under strong compositional effects, on top of the “balanced” simulation, we also select two highly abundant OTUs ( $\pi = 0.168$  and  $0.083$  respectively) to be differentially abundant in one group. We then apply DESeq2 on the simulated datasets with RLE, GMPR and TSS normalization, where we denote DESeq2-GMPR, DESeq2-RLE, DESeq2-TSS for these three approaches. For each approach, the P-values are calculated for each OTU and corrected for multiple testing using false discovery rate (FDR) control (Benjamini-Hochberg procedure). We evaluate the performance based on FDR control and ROC analysis, where the true positive rate is plotted against false positive rate at different P-value cutoffs. The observed FDR is calculated as

$$\frac{FP}{\max(1, FP + TP)},$$

159 where  $FP$  and  $TP$  are the number of false and true positives respectively. Simulation results are averaged  
 160 over 100 repetitions.

## 161 RESULTS

### 162 Simulation: GMPR is robust to differential and outlier OTUs

163 We first study the robustness of GMPR to differentially abundant OTUs and sample-specific outlier OTUs  
 164 by using the perturbation-based simulation approach, where we artificially alter the abundances of a  
 165 “fixed” or “random” set of OTUs under different levels of zero-inflation, percentage of perturbed OTUs  
 166 and strength of perturbation.

167 In the simulation of “fixed” perturbation (Figure 3), the performance of all methods decrease in most  
 168 cases with the increased zero percentage. TSS has excellent performance under moderate perturbation but  
 169 performs poorly under strong perturbation. GMPR, followed by CSS, consistently outperforms the other  
 170 methods when the perturbation is strong. When the perturbation is moderate, GMPR is only secondary to  
 171 TSS when the percentage of zeros is high (80%) and on par with TSS when the percentage of zeros is  
 172 moderate (70%) or low (60%). For RNA-Seq based methods, TMM performs better than RLE in either  
 173 strong or moderate perturbation. Though the performance of RLE+ improves by adding pseudo-counts to  
 174 the OTU data, the size factor estimated by TMM+ merely correlates with true library size when the zero  
 175 percentage is high (70% and 80%). In contrast, GMPR, together with CSS, performs stable in all cases  
 176 and GMPR yields better size factor estimate than CSS.

177 In the “random” perturbation scenario (Figure 4), performance of all methods decreases with the  
 178 increased zero percentage as the “fixed” scenario. Similar to the performance in “fixed” perturbation  
 179 scenario, TSS has excellent performance under moderate perturbation but performs poorly under strong  
 180 perturbation. When the perturbation is strong, GMPR, followed by CSS, still outperforms the other  
 181 methods. RNA-Seq based methods including TMM, TMM+, RLE and RLE+ have a similar trend as in  
 182 “fixed” perturbation. However, compared to “fixed” perturbation, the performance of TMM and RLE  
 183 decreases more obviously as the number of perturbed OTUs increases. In contrast, GMPR and CSS are  
 184 more robust to sample-specific outlier OTUs in all cases and GMPR results in better size factor estimate  
 185 than CSS.

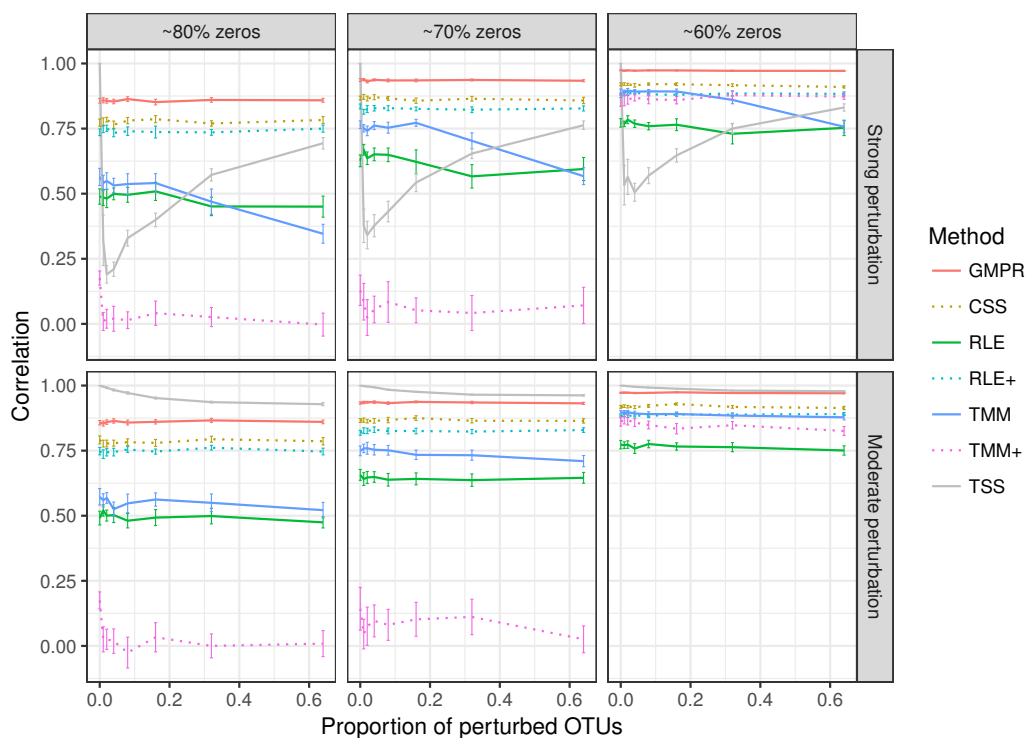


**Figure 3.** Spearman's correlation between the estimated size factors and the simulated "true" library sizes when a fixed set of OTUs are perturbed. The performance of different normalization methods are compared under different levels of zero-inflation, percentage of perturbed OTUs and strength of perturbation. Error bars represent 95% CIs.

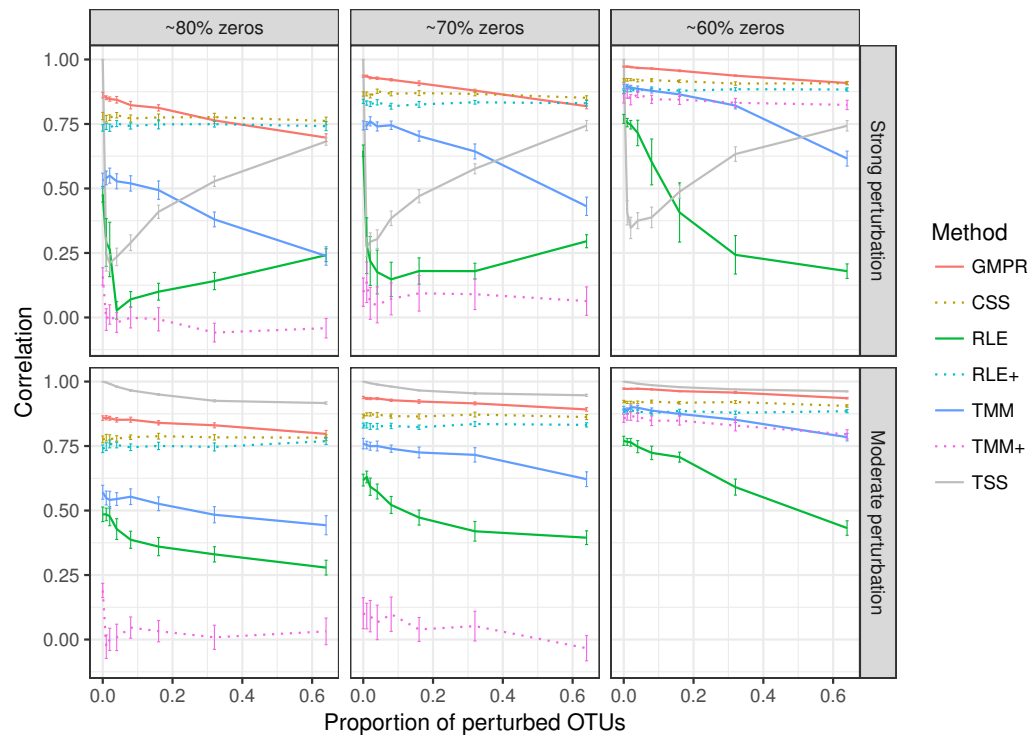


**Figure 4.** Spearman's correlation between the estimated size factors and the simulated "true" library sizes when a random set of OTUs are perturbed. The performance of different normalization methods are compared under different levels of zero-inflation, percentage of perturbed OTUs and strength of perturbation. Error bars represent 95% CIs.

**186 Simulation: GMPR improves the performance of differential abundance analysis**

187 In the previous section, we demonstrate that GMPR could better recover the “true” library size in  
188 presence of differentially abundant OTUs or sample-specific outlier OTUs. In this section, with a different  
189 perspective, we show that the robustness of GMPR method translates into a better false positive control  
190 and higher statistical power in the context of differential abundance analysis (DAA), where the aim is to  
191 detect differentially abundant OTUs between two sample groups.

192 We simulate the zeroinflated count data using ZINB model and use DESeq2 to perform DAA with  
193 different normalization schemes (RLE, GMPR and TSS). In one scenario, we randomly select 5% OTUs  
194 to be differential with a fold change of 4 in either sample group (Scene 1). In the other scenario, in  
195 addition to the 5% randomly selected OTUs, we select two highly abundant OTUs to be differentially  
196 abundant in one group to create strong compositional effects (Scene 2). In this scenario, the abundance  
197 change of these highly abundant OTUs will lead to the change of the “relative” abundances of other OTUs  
198 if the TSS normalization is used. The results for the two scenarios are presented in Figure 5. In Scene 1  
199 (Figure 5A-B), although all approaches have slightly elevated FDRs relative to the nominal levels (Figure  
200 5A), the observed FDR of DESeq2 using GMPR is closer to the nominal level than that using RLE (native  
201 normalization) and TSS. In terms of ROC-based power analysis (Figure 5B), GMPR achieves a higher  
202 AUC (Area Under the Curve) than RLE and TSS. In this “balanced” scenario, TSS performs relatively  
203 well and is even slightly better than RLE. The performance differences are more revealing in Scene 2  
204 (Figure 5C-D), where we artificially alter the abundances of two highly abundant OTUs. In this setting,  
205 TSS has a poor FDR control due to strong compositional effects and has a much lower statistical power at  
206 the same false positive rate. In contrast, the performance of GMPR and RLE remains stable, and GMPR  
207 performs better than RLE in terms of both FDR control and power.

**208 Real data: GMPR reduces the inter-sample variability of normalized abundances**

209 We next evaluate various normalization methods using 38 gut microbiome datasets from 16S rDNA  
210 sequencing of stool samples (Supplementary Table 1). These experimental datasets were retrieved from  
211 qiita database (<https://qiita.ucsd.edu/>) with a sample size larger than 50 each. The 38 datasets come from  
212 different species as well as a wide range of biological conditions. If a study involves multiple species,  
213 we include samples from the predominant species. We focus the analysis on gut microbiome samples  
214 because the gut microbiome is more studied than that from other sample types.

215 For the real data, it is not feasible to calculate the correlation between estimated size factors and  
216 “true” library sizes as done for simulations. As an alternative, we use the inter-sample variability as  
217 a performance measure since an appropriate normalization method will reduce the variability of the  
218 normalized OTU abundances (raw counts divided by the size factor) due to different library sizes. A  
219 similar measure has been used in the evaluation of normalization performance for microarray data (Fortin  
220 et al., 2014). We use the traditional variance as the metric to assess inter-sample variability. For each  
221 method, the variance of the normalized abundance of each OTU across all samples is calculated and the  
222 median of the variances of all OTUs or stratified OTUs (based on their prevalence) is reported for each  
223 study. For each study, all methods are ranked based on these median variances. The distributions of their  
224 ranks across these 38 studies for each method are depicted in Figure 6. A higher ranking (lower values in  
225 the box plot) indicates a better performance in terms of minimizing inter-sample variability.

226 In Figure 6, we could see that GMPR achieves the best performance with top ranks in 22 out of 38  
227 datasets, followed by CSS, which tops in 7 datasets (Supplementary Table 2). This result is consistent  
228 with the simulation studies, where GMPR and CSS are overall more robust to perturbations than other  
229 methods. Moreover, GMPR consistently performs the best for reducing the variability of OTUs at different  
230 prevalence level. It is also noticeable that the inter-sample variability is the largest without normalization  
231 (RAW) and TSS does not perform well for a large number of studies. As expected, RLE only works  
232 for 8 out of 38 datasets due to a large percentage of zero read counts. By adding pseudo-counts, RLE+  
233 improves the performance significantly compared to RLE. However, there is not much improvement of  
234 TMM+ compared to TMM. To see if the difference is significant, we performed paired Wilcoxon signed-  
235 rank tests between the ranks of the 38 datasets obtained by GMPR and by any other methods. GMPR  
236 achieves significantly better ranking than other methods (P-value < 0.05 for all OTUs or stratified OTUs).  
237 Supplementary Figure 1 compares the distributions of the OTU variances and their ranks for an example  
238 dataset (study ID 1561, all OTUs). Each OTU is ranked based on its variances among the competing  
239 methods. Although the difference in median variance is moderate, GMPR performs significantly better

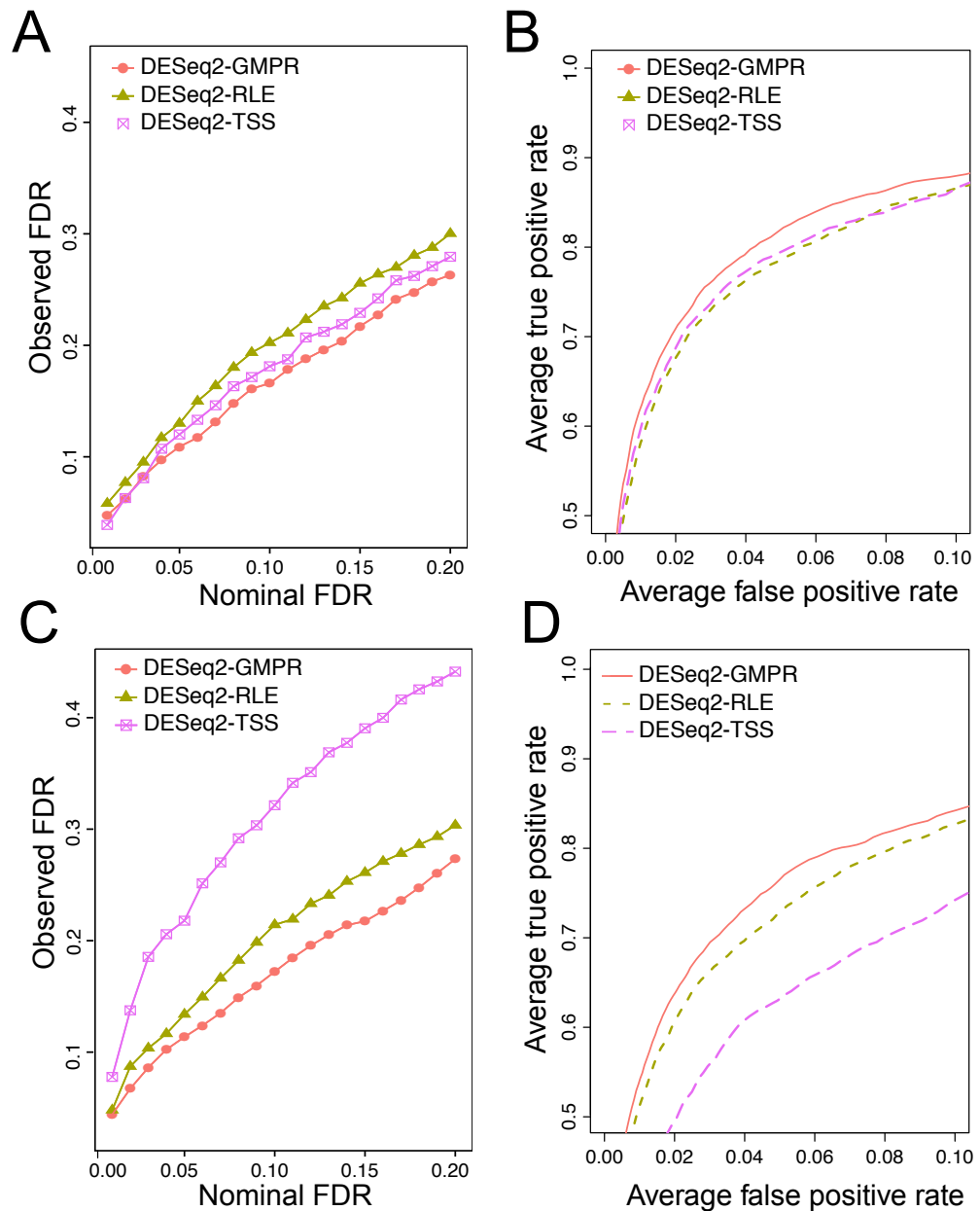


**Figure 5.** Comparison of the performance of different normalization schemes in DESeq2-based differential abundance analysis. A-B: Scene 1 ("balanced" scenario), 5% random OTUs are differentially abundant between two groups with a fold change of 4. C-D: Scene 2 ("unbalanced" scenario), in addition to 5% random OTUs, two highly abundant OTUs are differential abundant in one group to create strong compositional effects. A, C: ability to control the FDR. The observed FDR is plotted against the nominal FDR level. B, D: ROC curves to compare the power. The true positive rate is plotted against false positive rate at different P-value cutoffs.

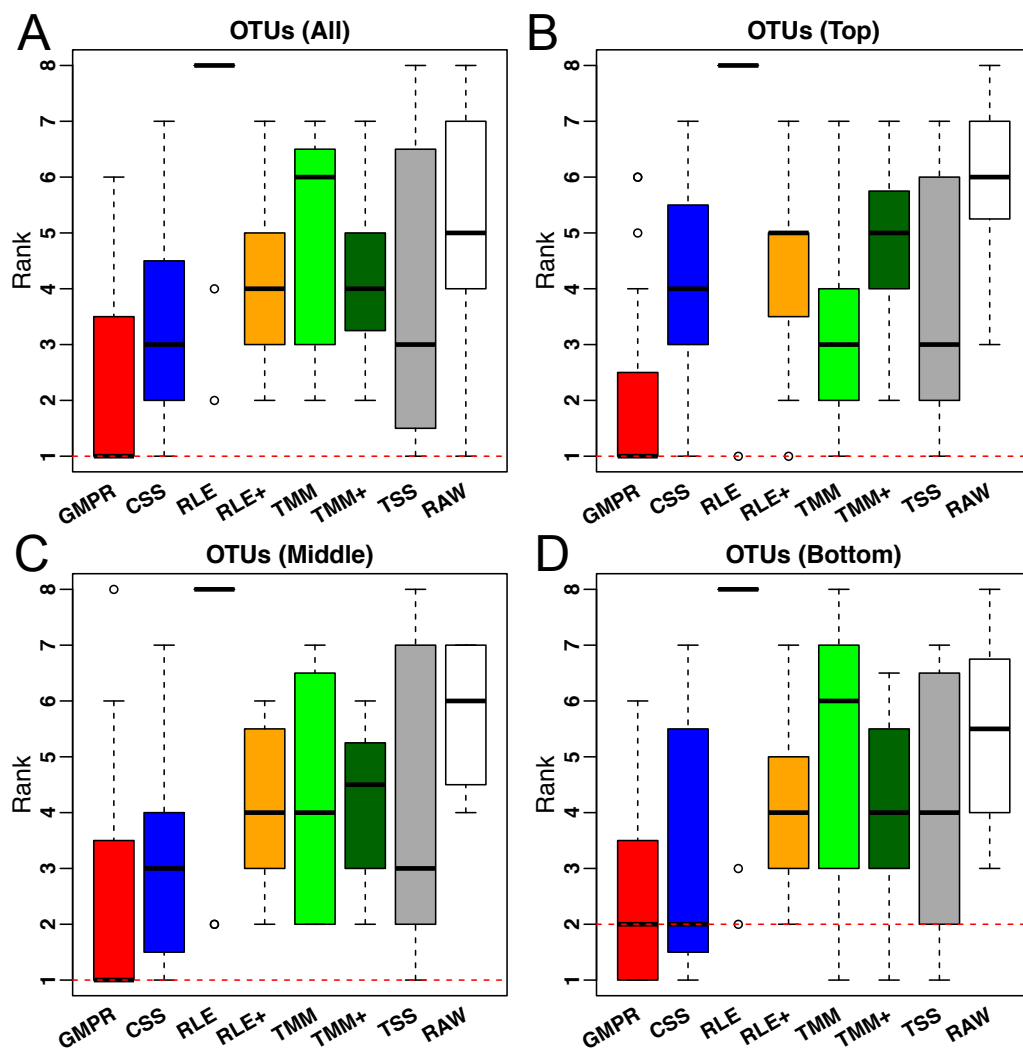


**Figure 6.** Comparison of normalization methods in reducing inter-sample variability of normalized OTU abundances based on 38 gut microbiome datasets. Distribution of the ranks for the medians of the OTU variances over the 38 datasets. The median is calculated over all OTUs (A) or OTUs of different prevalence level (B-C: Top, middle and bottom)

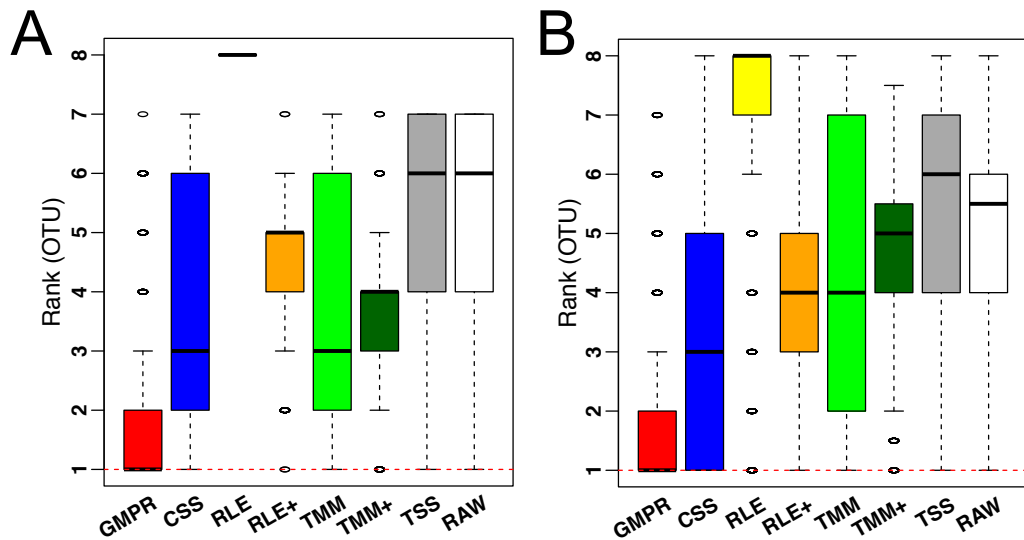


**Figure 7.** Comparison of normalization methods in reducing inter-sample variability of normalized OTU abundances based on an oral (A) and a skin (B) microbiome dataset. Distributions of the OTU ranks (each OTU is ranked based on its variances among the competing methods) are shown.

240 than other methods ( $P < 0.05$ , for all comparisons) and achieves a much lower rank.

241 To demonstrate the performance on low-diversity microbiome samples, we perform the same analyses  
 242 on an oral and a skin microbiome dataset from qiita (Supplementary Table 1, bottom). Based on the OTU  
 243 rank distribution (each OTU is ranked based on its variances among the competing methods), GMPR  
 244 achieves the lowest rank for majority of the OTUs, followed by CSS. The result is consistent with the  
 245 performance for gut microbiome datasets (Figure 7).

#### 246 **Real data: GMPR improves the reproducibility of normalized abundances**

247 When replicates are available, we could evaluate the performance of normalization based on its ability to  
 248 reduce between-replicate variability. Normalization will increase the reproducibility of the normalized  
 249 OTU abundances. In this section, we compare the performance of different normalization methods based  
 250 on a reproducibility analysis of a fecal stability study, which aims to compare the temporal stability of  
 251 different stool collection methods (Sinha et al., 2016). In this study, 20 healthy volunteers provided the  
 252 stool samples and these samples were subject to different treatment methods. The stool samples were  
 253 then frozen immediately or after storage in ambient temperature for one or four days for the study of  
 254 the stability of the microbiota. Each sample had two to three replicates for each condition and thus we  
 255 could perform reproducibility analysis based on the replicate samples. We evaluate the reproducibility  
 256 for the “no additive” treatment method for the data generated at Knight lab (Sinha et al., 2016), where  
 257 the stool samples were left untreated. Under this condition, certain bacteria will grow in the ambient  
 258 temperature with varying growth rates and we thus expect a lower agreement between replicates after  
 259 four-day ambient temperature storage.

We conduct the reproducibility analysis on the core genera, which are present in more than 75%  
 samples (a total of 26 genera are assessed). We first estimate the size factors based on the OTU-level  
 data and the genus-level counts are divided by the size factors to produce normalized genus-level  
 abundances. Intraclass correlation coefficients (ICC) is used to quantify the reproducibility for the  
 genus-level normalized abundances. The ICC is defined as,

$$\rho = \frac{\sigma_b^2}{\sigma_b^2 + \sigma_e^2}$$

260 where  $\sigma_b^2$  represents the biological variability, i.e., sample-to-sample variability and  $\sigma_e^2$  represents the  
 261 replicate-to-replicate variability. We calculate the ICC for 26 core genera for “day 0” (immediately frozen)

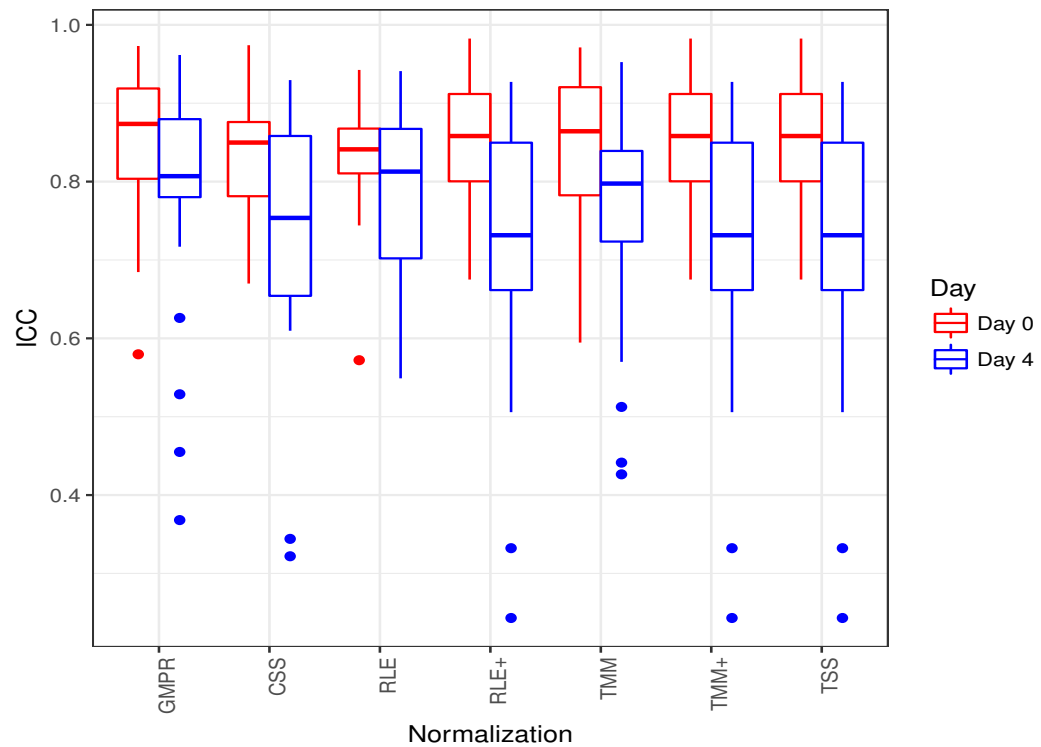


**Figure 8.** ICC as a measurement for reproducibility is calculated for 26 core genera normalized by different methods for “day 0” and “day 4” respectively.

262 and “day 4” (frozen after four-day storage) respectively. The ICCs are estimated using the R package  
 263 “ICC” based on the mixed effects model. An ICC closer to one indicates excellent reproducibility.

264 Figure 8 shows that the reproducibility of the genera in “day 0” has higher reproducibility than “day  
 265 4” regardless of the normalization method used since reproducibility decreases as certain bacteria grow  
 266 randomly as time elapses. While all the methods have resulted in comparable ICCs for “day 0”, GMPR  
 267 achieves higher ICCs for “day 4” than the rest methods. Sinha et al. (2016) showed that most taxa were  
 268 relatively stable over 4 days and only a small group of taxa (mostly OTUs from *Gammaproteobacteria*)  
 269 displayed a pronounced growth at ambient temperature. This suggests that most of the genera may be  
 270 temporally stable and their “day 4” ICCs should be close to the “day 0” ICCs. However, due to the  
 271 compositional effect, if the data are not properly normalized, a few fast-growing bacteria will skew the  
 272 relative abundances of other bacteria, leading to apparently lower ICCs for those stable genera. In contrast,  
 273 the GMPR method is more robust to differential or outlier taxa as demonstrated by the simulation study,  
 274 which explains higher ICCs for “day 4” samples.

## 275 CONCLUSION AND DISCUSSION

276 Normalization is a critical step in processing microbiome data, rendering multiple samples comparable by  
 277 removing the bias caused by variable sequencing depths. Normalization paves the way for the downstream  
 278 analysis, especially for differential abundance analysis of microbiome data, where proper normalization  
 279 could reduce the false positive rates due to compositional effects. However, the characteristics of  
 280 microbiome sequencing data, including over-dispersion and zero-inflation, make the normalization a  
 281 non-trivial task.

282 In this study, we propose the GMPR method for normalizing microbiome sequencing data by address-  
 283 ing the zero-inflation. In one simulation study, we demonstrate GMPR’s effectiveness by showing it  
 284 performs better than other normalization methods in recovering the original library sizes when a subset  
 285 of OTUs are differentially abundant or when random outlier OTUs exist. In another simulation study,  
 286 GMPR yields better FDR control and higher power in detecting differentially abundant OTUs. In real data  
 287 analysis, we show GMPR reduces the inter-sample variability and increases inter-replicate reproducibility

288 of normalized taxa abundances. Overall, GMPR outperforms RNA-Seq normalization methods including  
289 TMM and RLE and modified TMM+ and RLE+. It also yields better performance than CSS, which is a  
290 normalization method specifically designed for microbiome data. As a general normalization method for  
291 zero-inflated sequencing data, GMPR could also be applied to other sequencing data with excessive zeros  
292 such as single-cell RNA-Seq data (Vallejos et al., 2017).

293 We note that the main application of GMPR method is for taxon-level analysis such as the presented  
294 differential abundance analysis and reproducibility analysis, where it is important to distinguish those  
295 “truly” differential from “falsely” differential taxa due to compositional effects. Although we could apply  
296 the proposed normalization to (weighted) distance-based statistical methods such as ordination, clustering  
297 and PERMANOVA (Caporaso et al., 2010; Chen et al., 2012) based on the GMPR-normalized abundance  
298 data, simulations show that the advantage of using GMPR is very limited for such applications, compared  
299 to the traditionally used TSS method (i.e., proportion-based method) (Supplementary Figure 2). This  
300 is explained by the fact that the distance-based analysis focuses on the overall dissimilarity and the  
301 proportional data is already efficient enough to capture the overall dissimilarity. Probably, more important  
302 factors to consider in distance-based statistical methods are the selection of the most relevant distance  
303 measure and/or the application of appropriate transformation after normalization (Costea et al., 2014;  
304 Thorsen et al., 2016).

305 Besides the size factor-based approach (GMPR, CSS, TSS, RLE, TMM), the other popular approach  
306 for normalizing the microbiome data is through rarefaction. Both approaches have weakness and  
307 strength for particular applications. Although rarefaction discards a significant portion of the reads and  
308 is probably not optimal from an information perspective, it is still widely used for microbiome data  
309 analysis, particularly for  $\alpha$ - and  $\beta$ -diversity analysis. The reason for its extensive use is that the majority  
310 of the taxa in the microbiota are of low abundance and their presence/absence strongly depends on the  
311 sequencing depth. Thus rarefaction puts the comparison of  $\alpha$ - and  $\beta$ -diversity on an equal basis. Size  
312 factor-based normalization, on the other hand, is unable to address this problem. Thus rarefaction is still  
313 recommended for  $\alpha$ - and  $\beta$ -diversity analysis, especially for unweighted measures and for confounded  
314 scenarios, where the sequencing depth correlates with the variable of interest (Weiss et al., 2017). For  
315 differential abundance analysis, one major challenge is to address the compositional problem. Rarefaction  
316 has a limited ability in this regard since the total sum constraint still exists after rarefaction. In addition, it  
317 suffers from a great power loss due to the discard of a large number of reads (McMurdie and Holmes,  
318 2014). In contrast, the size factor-based approaches are capable of capturing the invariant part of the taxa  
319 counts and address the compositional problem efficiently through normalization by the size factors. The  
320 size factors could be naturally included as offsets in count-based parametric models to address uneven  
321 sequencing depth (Chen et al., 2018).

322 GMPR is an inter-sample normalization method and has a computational complexity of  $O(n^2q)$ , where  
323  $n$  and  $q$  are the number of samples and features respectively. While GMPR calculates the size factors  
324 for a typical microbiome dataset ( $n < 1000$ ) in seconds, it does not scale linearly with the sample size.  
325 Large samples sizes are increasingly popular for epidemiological study and genetic association study of  
326 the microbiome (Robinson et al., 2016; Hall et al., 2017), where tens or hundreds of thousands of samples  
327 will be collected to detect weak association signals. For such large sample sizes, GMPR may take a much  
328 longer time. A potential strategy for efficient computation under ultra-large sample sizes is to divide the  
329 dataset into overlapping blocks, calculate GMPR size factors on these blocks and unify the size factors  
330 through the overlapping samples between blocks. To increase the computational efficiency of GMPR for  
331 ultra-large sample sizes will be the focus of our future research.

## 332 REFERENCES

- 333 Aird, D., Ross, M. G., Chen, W.-S., Danielsson, M., Fennell, T., Russ, C., Jaffe, D. B., Nusbaum, C., and  
334 Gnirke, A. (2011). Analyzing and minimizing PCR amplification bias in illumina sequencing libraries.  
335 *Genome Biol*, 12(2):R18.
- 336 Anders, S. and Huber, W. (2010). Differential expression analysis for sequence count data. *Genome Biol.*,  
337 11(10):R106.
- 338 Caporaso, J. G., Kuczynski, J., Stombaugh, J., Bittinger, K., Bushman, F. D., Costello, E. K., Fierer, N.,  
339 Peña, A. G., Goodrich, J. K., Gordon, J. I., Huttley, G. A., Kelley, S. T., Knights, D., Koenig, J. E.,  
340 Ley, R. E., Lozupone, C. A., McDonald, D., Muegge, B. D., Pirrung, M., Reeder, J., Sevinsky, J. R.,

- 341 Turnbaugh, P. J., Walters, W. A., Widmann, J., Yatsunencko, T., Zaneveld, J., and Knight, R. (2010).  
342 Qiime allows analysis of high-throughput community sequencing data. *Nat Methods*, 7(5):335–6.
- 343 Chen, J., Bittinger, K., Charlson, E. S., Hoffmann, C., Lewis, J., Wu, G. D., Collman, R. G., Bushman,  
344 F. D., and Li, H. (2012). Associating microbiome composition with environmental covariates using  
345 generalized unifracs distances. *Bioinformatics*, 28(16):2106–13.
- 346 Chen, J., King, E., Deek, R., Wei, Z., Yu, Y., Grill, D., and Ballman, K. (2018). An omnibus test for  
347 differential distribution analysis of microbiome sequencing data. *Bioinformatics*, 34(4):643–51.
- 348 Chen, J. and Li, H. (2013). Variable selection for sparse dirichlet-multinomial regression with an  
349 application to microbiome data analysis. *Ann. Appl. Stat.*, 7(1).
- 350 Costea, P. I., Zeller, G., Sunagawa, S., and Bork, P. (2014). A fair comparison. *Nat Methods*, 11(4):359.
- 351 Dillies, M.-A., Rau, A., Aubert, J., Hennequet-Antier, C., Jeanmougin, M., Servant, N., Keime, C., Marot,  
352 G., Castel, D., Estelle, J., Guernec, G., Jagla, B., Jouneau, L., Laloë, D., Le Gall, C., Schaëffer, B.,  
353 Le Crom, S., Guedj, M., Jaffrézic, F., and French StatOmique Consortium (2013). A comprehensive  
354 evaluation of normalization methods for illumina high-throughput rna sequencing data analysis. *Brief*  
355 *Bioinform*, 14(6):671–83.
- 356 Fortin, J., Labbe, A., Lemire, M., Zanke, B., Hudson, T., and Fertig, E. (2014). Functional normalization  
357 of 450k methylation array data improves replication in large cancer studies. *Genome Biol.*, 15(11):503.
- 358 Hall, A. B., Tolonen, A. C., and Xavier, R. J. (2017). Human genetic variation and the gut microbiome in  
359 disease. *Nat Rev Genet*, 18(11):690–699.
- 360 Li, P., Piao, Y., Shon, H. S., and Ryu, K. H. (2015). Comparing the normalization methods for the  
361 differential analysis of illumina high-throughput rna-seq data. *BMC Bioinformatics*, 16:347.
- 362 Love, M. I., Huber, W., and Anders, S. (2014). Moderated estimation of fold change and dispersion for  
363 rna-seq data with deseq2. *Genome Biol*, 15(12):550.
- 364 Mandal, S., Van Treuren, W., White, R. A., Eggesbø, M., Knight, R., and Peddada, S. D. (2015). Analysis  
365 of composition of microbiomes: a novel method for studying microbial composition. *Microb Ecol*  
366 *Health Dis*, 26(1):27663.
- 367 McMurdie, P. J. and Holmes, S. (2014). Waste not, want not: why rarefying microbiome data is  
368 inadmissible. *PLoS Comput Biol*, 10(4):e1003531.
- 369 Morton, J. T., Sanders, J., Quinn, R. A., McDonald, D., Gonzalez, A., Vázquez-Baeza, Y., Navas-Molina,  
370 J. A., Song, S. J., Metcalf, J. L., Hyde, E. R., Lladser, M., Dorrestein, P. C., and Knight, R. (2017).  
371 *mSystems*, 2(1):e00162–16.
- 372 Paulson, J., Stine, O., Bravo, H., and Pop, M. (2013). Differential abundance analysis for microbial  
373 marker-gene surveys. *Nat. methods*, 10(12):1200–1202.
- 374 Robinson, C. K., Brotman, R. M., and Ravel, J. (2016). Intricacies of assessing the human microbiome in  
375 epidemiologic studies. *Ann Epidemiol*, 26(5):311–21.
- 376 Robinson, M. D., McCarthy, D. J., and Smyth, G. K. (2010). edgeR: a bioconductor package for differential  
377 expression analysis of digital gene expression data. *Bioinformatics*, 26(1):139–40.
- 378 Robinson, M. D. and Oshlack, A. (2010). A scaling normalization method for differential expression  
379 analysis of rna-seq data. *Genome Biol.*, 11(3):R25.
- 380 Sinha, R., Chen, J., Amir, A., Vogtmann, E., Shi, J., Inman, K. S., Flores, R., Sampson, J., Knight, R., and  
381 Chia, N. (2016). Collecting fecal samples for microbiome analyses in epidemiology studies. *Cancer*  
382 *Epidemiol Biomarkers Prev*, 25(2):407–16.
- 383 Thorsen, J., Brejnrod, A., Mortensen, M., Rasmussen, M. A., Stokholm, J., Al-Soud, W. A., Sørensen,  
384 S., Bisgaard, H., and Waage, J. (2016). Large-scale benchmarking reveals false discoveries and count  
385 transformation sensitivity in 16s rRNA gene amplicon data analysis methods used in microbiome studies.  
386 *Microbiome*, 4(1):62.
- 387 Tsilimigras, M. C. and Fodor, A. A. (2016). Compositional data analysis of the microbiome: fundamentals,  
388 tools, and challenges. *Ann Epidemiol*, 26(5):330–5.
- 389 Vallejos, C. A., Risso, D., Scialdone, A., Dudoit, S., and Marioni, J. C. (2017). Normalizing single-cell  
390 rna sequencing data: challenges and opportunities. *Nat Methods*, 14(6):565–571.
- 391 Wang, Z., Gerstein, M., and Snyder, M. (2009). Rna-seq: a revolutionary tool for transcriptomics. *Nat*  
392 *Rev Genet*, 10(1):57–63.
- 393 Weiss, S., Xu, Z. Z., Peddada, S., Amir, A., Bittinger, K., Gonzalez, A., Lozupone, C., Zaneveld, J. R.,  
394 Vázquez-Baeza, Y., Birmingham, A., Hyde, E. R., and Knight, R. (2017). Normalization and microbial  
395 differential abundance strategies depend upon data characteristics. *Microbiome*, 5(1):27.

396 Wu, G. D., Chen, J., Hoffmann, C., Bittinger, K., Chen, Y. Y., Keilbaugh, S. A., Bewtra, M., Knights, D.,  
397 Walters, W. A., Knight, R., Sinha, R., Gilroy, E., Gupta, K., Baldassano, R., Nessel, L., Li, H., Bushman,  
398 F. D., and Lewis, J. D. (2011). Linking long-term dietary patterns with gut microbial enterotypes.  
399 *Science*, 334(6052):105–108.